physical sciences forum

MDPI

Proceeding Paper

Atomic Structure Analysis and Radiative Properties with Einstein Coefficients for Ne-like Se (Se XXV) †

Malvika Singh *, Richa Paijwar and Rinku Sharma

Department of Applied Physics, Delhi Technological University, Delhi 110042, India; richagautam2001@gmail.com (R.P.); rinkusharma@dtu.ac.in (R.S.)

* Correspondence: malvikasingh5995@gmail.com

† Presented at the 1st International Online Conference on Atoms, 29–30 January 2026; Available online: https://sciforum.net/event/IOCAT2026.

Abstract

We present a detailed study of the atomic structure and radiative properties of highly charged neon-like selenium (Se XXV), motivated by its importance in plasma diagnostics, fusion research, and astrophysical spectroscopy. We calculated excitation energies and radiative parameters for the 50 lowest levels of fine structure using a fully relativistic multiconfiguration Dirac–Fock approach. We calculated transition wavelengths, radiative transition rates, oscillator strengths, and line strengths for electric dipole, magnetic dipole, electric quadrupole, and magnetic quadrupole transitions among the specified levels. We also evaluated Einstein coefficients for spontaneous and stimulated emission, transition dipole moments, and radiative lifetimes of the low-lying states. To validate the results, we performed independent relativistic calculations using an alternative theoretical method and compared the datasets to examine internal consistency. The calculated excitation energies and radiative parameters agree well with values reported in the National Institute of Standards and Technology database (NIST) and other published theoretical results. The agreement between the independent approaches confirms the consistency of the present dataset. These results provide reliable atomic data for spectral line identification and quantitative plasma modeling in laboratory and astrophysical environments and support ongoing experimental and diagnostic studies of highly charged ions.

Keywords: radiative transition rates; Einstein coefficients; plasma diagnostics; spectral modeling

1. Introduction

Highly charged ions play an important role in laboratory and astrophysical plasmas. Their spectral lines provide essential diagnostics of plasma temperature, electron density, and ionization balance. Accurate atomic structure and radiative data are therefore necessary for interpreting spectra from inertial confinement fusion experiments, magnetic confinement fusion devices, laser-produced plasmas, and solar and astrophysical sources. Medium- and high-Z elements frequently appear as intrinsic or injected impurities in fusion plasmas, which increases the need for reliable atomic datasets.

Neon-like ions attract considerable interest because their closed-shell ground configuration ($1s^2 2s^2 2p^6$) provides structural stability while retaining strong relativistic and electron-correlation effects. Their resonance and intercombination transitions serve as important plasma diagnostic lines. Recent high-precision spectroscopic measurements of

Check for updates

Academic Editor: Omar Ariel Fojón

Published: 13 May 2026

Copyright: © 2026 by the authors. Licensee MDPI, Basel, Switzerland. This article is an open access article distributed under the terms and conditions of the Creative Commons Attribution (CC BY) license.

neon-like highly charged ions using electron beam ion traps and synchrotron radiation sources demonstrate continued experimental efforts to benchmark theoretical predictions. Despite these advances, comprehensive and systematically validated radiative datasets for neon-like selenium (Se XXV) remain relatively limited [1,2].

Selenium plays a role in plasma research. Experimental studies have injected selenium [3] as a diagnostic impurity in tokamak plasmas [4] to establish wavelength standards and to study impurity transport. Selenium has also been used in soft X-ray laser development experiments [5]. Several investigations have examined sodium-like selenium (Se XXIV) using model potential methods, Hartree–Slater approaches, many-body perturbation theory, and multiconfiguration techniques; however, comparatively limited systematic studies have focused on the detailed radiative properties and low-lying levels of neon-like Se XXV [6,7].

The reliability of atomic data for highly charged ions depends on the treatment of relativistic effects, electron correlation, and quantum electrodynamic contributions. We therefore examine whether independent relativistic multiconfiguration approaches yield consistent excitation energies and transition probabilities for Ne-like Se XXV, thereby providing dependable input for plasma diagnostics and modeling [8].

In this study, we calculated the relativistic atomic structure of the 50 lowest fine-structure levels of neon-like selenium (Se XXV) [9]. We determined transition wavelengths, oscillator strengths, line strengths, Einstein coefficients, and radiative lifetimes for electric dipole, magnetic dipole, electric quadrupole, and magnetic quadrupole transitions. We also carried out independent relativistic calculations to assess internal consistency. The calculated parameters show agreement with available reference data and provide atomic data for spectral diagnostics and plasma modeling applications [10,11].

2. Materials and Methods

2.1. Relativistic Multiconfiguration Dirac–Fock Method

We performed fully relativistic atomic structure calculations for neon-like Se XXV using the multiconfiguration Dirac–Fock (MCDF) method within the Dirac–Coulomb framework. We constructed N-electron atomic state functions as linear combinations of configuration state functions with defined total angular momentum and parity [12].

We included electron correlation effects through configuration interaction among configurations associated with the lowest 50 fine-structure levels. The relativistic formalism accounts for spin–orbit coupling and other relativistic contributions arising from the Dirac treatment of the atomic Hamiltonian. We optimized orbital functions self-consistently to achieve convergence of excitation energies and radiative parameters.

2.2. Flexible Atomic Code (FAC)—Interaction Calculations

To examine the robustness and internal consistency of the calculated data, we carried out independent, fully relativistic configuration–interaction calculations based on a Dirac–Fock–Slater central-field potential. In this approach, we generated one-electron orbitals in a self-consistent local potential that includes contributions from the nuclear charge and electron–electron interactions.

Unlike the MCDF method, which variationally optimizes orbitals for selected states, the Dirac–Fock–Slater approach uses a central-field approximation and provides an alternative description of correlation effects and transition amplitudes [13]. We constructed the active space by including single and double electron excitations from the ground configuration $2s^2 2p^6$. The singly excited configurations consist of $2s^2 2p^5 nl$, and the core-excited configurations of the form $2s2p^6 nl$. The principal quantum number ranges $3 \leq n \leq 7$, with orbital angular momentum $l = s, p, d, f$. In addition, doubly excited configurations of the

type $2s^2 2p^4 nl\ n'l'$ (n = 3; L = n − 1) (n′ = 3, 4, 5; l′ = n′ − 1) were included to account for electron correlation effects. This choice of active space enables a balanced treatment of the valence and core–valence excitations for improving the accuracy and the convergence of the calculated atomic parameters.

The agreement between the two relativistic treatments serves as internal validation of the calculated excitation energies and radiative quantities.

2.3. Radiative Transition Parameters

Using the wavefunctions obtained from the relativistic calculations, we evaluated radiative transition parameters for the lowest 50 fine-structure levels of Ne-like Se XXV. We determined transition wavelengths, radiative transition probabilities, oscillator strengths, and line strengths for electric dipole (E1), magnetic dipole (M1), electric quadrupole (E2), and magnetic quadrupole (M2) transitions. We evaluated Einstein coefficients for spontaneous and stimulated emission for the considered transitions. For allowed transitions, we calculated transition dipole moments. We obtained radiative lifetimes of excited levels from the inverse of the total radiative decay rate, where the total rate includes contributions from all allowed E1, M1, E2, and M2 transitions from a given upper level. For E1 transitions, we evaluated radiative parameters in the length (Babushkin) gauge and used the agreement between length and velocity forms as an internal consistency check. For strong allowed transitions, the ratio between the two gauges approaches unity, whereas larger deviations occur mainly for weak transitions due to cancellation effects in the transition matrix elements. These quantities describe the spectroscopic properties and radiative behavior of the ion.

We assessed the accuracy of the calculations by comparing excitation energies, wavelengths, oscillator strengths, and line strengths with available tabulated data from the NIST atomic spectra database and previously reported theoretical data. For strong allowed transitions, the results show agreement, indicating that the adopted relativistic configuration–interaction treatments provide reliable atomic structure and radiative parameters for Ne-like Se XXV.

3. Results

3.1. Energy Levels

Table 1 lists the excitation energies and radiative lifetimes for the lowest 50 fine-structure levels of neon-like Se XXV. These levels arise mainly from the configurations $2p^6$, $2p^5 3s$, $2p^5 3p$, $2p^5 3d$, 2s3s, 2s3p, 2s3d, $2p^5 4s$, $2p^5 4p$, and $2p^5 4d$. The ground state corresponds to the closed-shell configuration $2p^6$ with total angular momentum J = 0, which defines the zero-energy reference level. The first excited levels belong to the $2p^5 3s$ configuration and appear at the excitation energy of around 1430 eV. Higher excited levels arise from the configurations $2p^5 3p$ and $2p^5 3d$ and extend the energy spectrum to larger excitation energies. To obtain reliable atomic data, we incorporated relativistic effects and configuration interaction in our atomic structure calculations. In the present work, we performed the calculations using two independent relativistic atomic-structure codes, namely, the Flexible Atomic Code (FAC) developed by Ming Feng Gu and the General-purpose Relativistic Atomic Structure Program (GRASP). Using these two independent methods provides an important internal consistency check for the calculated energies and other atomic parameters. A comparison of FAC and GRASP results reported in Table 1 shows excellent agreement. For most levels, the calculated excitation energies from the two codes are very similar, indicating that both computational approaches provide a reliable description of the relativistic atomic structure of the ion. The small deviations in the two sets of results could be due to the differences in the treatment of configuration interaction, the numerical procedures used to solve the Dirac equations, and the construction of radial

orbitals in the above two codes. Such differences are expected when independent theoretical methods are employed and are often used to assess the structural stability of calculated atomic configurations.

Table 1. Energies (in eV) for the lowest 50 levels and lifetime (in sec) of Ne-like Se.

Level No.	Configurations	P	J	FAC	GRASP	NIST	%Error (FAC)	%Error (GRASP)	Lifetime (s)
0	2p6	0	0	0	0	0			
1	2p5.3s1	1	2	1433.26	1433.42				
2	2p5.3s1	1	1	1436.32	1436.34	1439.21	0.20	0.20	2.45×10^{-13}
3	2p5.3s1	1	0	1475.75	1475.96				
4	2p5.3s1	1	1	1477.36	1477.49	1480.62	0.22	0.21	3.61×10^{-13}
5	2p5.3p1	0	1	1480.74	1480.81				1.42×10^{-10}
6	2p5.3p1	0	2	1483.92	1484.07				1.20×10^{-10}
7	2p5.3p1	0	3	1492.46	1492.52				6.87×10^{-11}
8	2p5.3p1	0	1	1493.09	1493.20				7.87×10^{-11}
9	2p5.3p1	0	2	1496.80	1496.99				5.74×10^{-11}
10	2p5.3p1	0	0	1510.28	1510.83				3.74×10^{-11}
11	2p5.3p1	0	1	1525.30	1525.46				1.26×10^{-10}
12	2p5.3p1	0	1	1535.90	1536.05				6.30×10^{-11}
13	2p5.3p1	0	2	1536.97	1537.14				6.57×10^{-11}
14	2p5.3p1	0	0	1547.12	1548.66				2.15×10^{-11}
15	2p5.3d1	1	0	1551.40	1551.67				4.82×10^{-11}
16	2p5.3d1	1	1	1553.44	1553.72	1556.25	0.18	0.16	3.51×10^{-12}
17	2p5.3d1	1	4	1556.99	1557.33	1574.50	1.11	1.09	4.31×10^{-11}
18	2p5.3d1	1	3	1557.00	1557.23	1613.28	3.49	3.47	5.92×10^{-11}
19	2p5.3d1	1	2	1557.22	1557.51				5.03×10^{-11}
20	2p5.3d1	1	2	1560.18	1560.53				4.45×10^{-11}
21	2p5.3d1	1	3	1562.64	1563.02				5.20×10^{-11}
22	2p5.3d1	1	1	1572.41	1573.10	1574.50	0.13	0.09	2.05×10^{-14}
23	2p5.3d1	1	2	1599.15	1599.44				4.21×10^{-11}
24	2p5.3d1	1	2	1601.29	1601.70				5.42×10^{-11}
25	2p5.3d1	1	3	1602.58	1603.00				5.52×10^{-11}
26	2p5.3d1	1	1	1610.67	1611.52	1613.28	0.16	0.11	1.31×10^{-14}
27	2s1.3s1	0	1	1650.38	1652.09				3.42×10^{-12}
28	2s1.3s1	0	0	1660.42	1662.75				4.97×10^{-12}
29	2s1.3p1	1	0	1699.24	1701.13				3.74×10^{-12}
30	2s1.3p1	1	1	1700.15	1702.02	1690.82	0.55	0.66	2.66×10^{-13}
31	2s1.3p1	1	2	1709.52	1711.36				3.61×10^{-12}
32	2s1.3p1	1	1	1712.12	1713.91	1711.73	0.02	0.13	7.41×10^{-14}
33	2s1.3d1	0	1	1770.85	1773.27				4.23×10^{-12}
34	2s1.3d1	0	2	1771.44	1773.86				4.12×10^{-12}
35	2s1.3d1	0	3	1772.74	1775.14				4.07×10^{-12}
36	2s1.3d1	0	2	1780.14	1782.64				3.92×10^{-12}
37	2p5.4s1	1	2	1941.99	1942.15				6.55×10^{-13}
38	2p5.4s1	1	1	1942.97	1943.13	1947.05	0.21	0.20	3.30×10^{-13}
39	2p5.4p1	0	1	1961.59	1961.79				6.23×10^{-13}
40	2p5.4p1	0	2	1962.43	1962.66				6.13×10^{-13}
41	2p5.4p1	0	3	1965.92	1966.13				6.62×10^{-13}
42	2p5.4p1	0	1	1966.22	1966.44				6.47×10^{-13}
43	2p5.4p1	0	2	1967.47	1967.71				6.78×10^{-13}
44	2p5.4p1	0	0	1973.91	1974.69				7.22×10^{-13}
45	2p5.4s1	1	0	1984.57	1984.77				6.51×10^{-13}
46	2p5.4s1	1	1	1984.98	1985.18	1961.18	1.21	1.22	3.07×10^{-13}
47	2p5.4d1	1	0	1988.39	1988.51				3.57×10^{-13}
48	2p5.4d1	1	1	1989.18	1989.32	1999.37	0.51	0.50	3.50×10^{-13}
49	2p5.4d1	1	3	1990.25	1990.47				3.62×10^{-13}
50	2p5.4d1	1	4	1990.39	1990.54				3.57×10^{-13}

We also compared the calculated energies with the values listed in the National Institute of Standards and Technology Atomic Spectra Database. This comparison shows that the theoretical results agree well with the experimental values. The percentage deviations shown in Table 1 indicate that the calculated energies closely follow the experimental trends, although some discrepancies appear for a few highly excited levels, which could be due to configuration mixing among nearby states or limitations in the configuration interaction expansion used in the calculations. Nevertheless, the overall close agreement between the theoretical calculations and the available experimental data indicates that the present results provide a good, reliable description of the low-lying energy structure of Neon-like Se XXV [14].

3.2. Radiative Lifetimes

We obtained radiative lifetimes for the low-lying levels from the inverse of the total radiative decay rate, including contributions from electric dipole, magnetic dipole, electric quadrupole, and magnetic quadrupole transitions. Including all multipole channels provides a complete description of level decay behavior. The inclusion of all multipole channels provides a complete description of the radiative decay behavior of the excited states. The calculated lifetimes are listed in Table 1.

Furthermore, we present a graphical comparison (Figure 1) of the calculated energies obtained from both codes with the NIST data, and the results exhibit good agreement with the standard reference values.

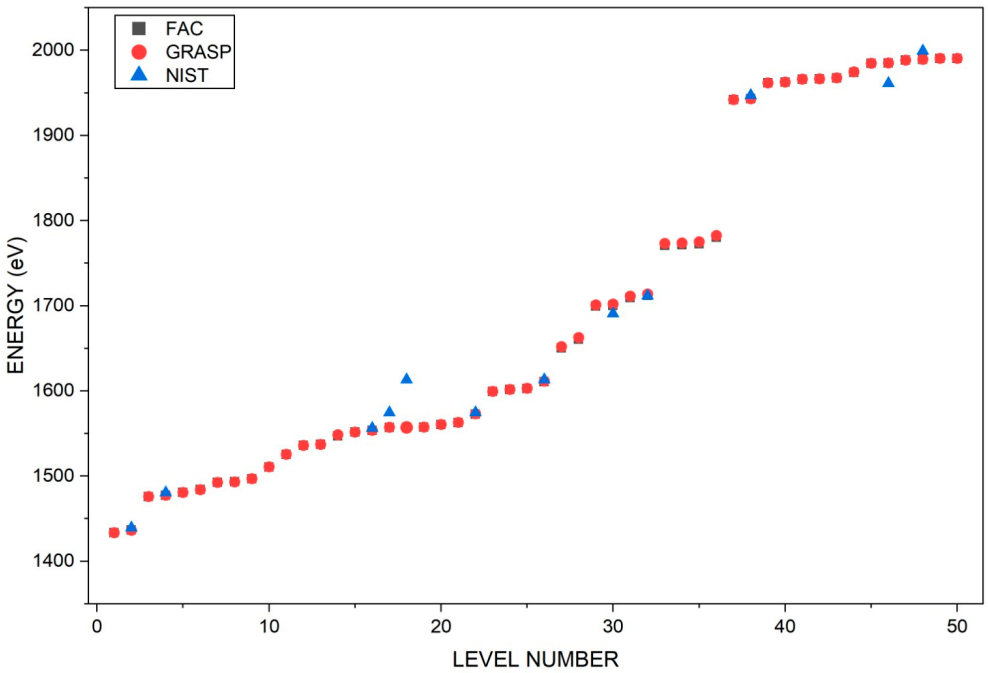

Figure 1. Graphical comparison of the present calculated energies with the NIST data [14].

3.3. Radiative Transition Parameters

Table 2 presents the radiative parameters for the electric-dipole (E1) transitions from several excited levels to the ground level of Neon-like Se. The table lists the transition wavelength, emission transition probability A_{ij}, absorption oscillator strength f_{ji}, and line strength S_{ij}. These quantities characterize the strength and probability of radiative transitions and provide valuable information about the spectroscopic properties of the ion.

Table 2. Radiative data for Ne-like Se, E1 transitions to ground state, A_{IJ}—emission transition probability (s^{-1}), F_{JI}—absorption oscillator strength, S_{IJ}—line-strength (a.u.).

I	J	Wavelength (Å)	A_{IJ} (s^{-1})	F_{JI}	S_{IJ}
2	0	8.63	4.08×10^{12}	1.37×10^{-1}	3.89×10^{-3}
4	0	8.39	2.77×10^{12}	8.78×10^{-2}	2.42×10^{-3}
16	0	7.98	2.64×10^{11}	7.57×10^{-3}	1.99×10^{-4}
22	0	7.88	4.88×10^{13}	1.36×10^{0}	3.54×10^{-2}
26	0	7.69	7.64×10^{13}	2.03×10^{0}	5.15×10^{-2}
30	0	7.28	3.49×10^{12}	8.33×10^{-2}	2.00×10^{-3}
32	0	7.23	1.32×10^{13}	3.11×10^{-1}	7.40×10^{-3}
38	0	6.38	1.48×10^{12}	2.71×10^{-2}	5.70×10^{-4}
46	0	6.25	1.69×10^{12}	2.97×10^{-2}	6.11×10^{-4}
48	0	6.23	6.55×10^{10}	1.14×10^{-3}	2.35×10^{-5}

The calculated transition wavelengths shown in Table 2 for the considered transitions lie in the range of approximately 6.23–8.63 Å, corresponding to soft X-ray spectral lines associated with highly charged neon-like ions. The emission transition probabilities span several orders of magnitude, ranging from about 10^{10} s^{-1} to 10^{13} s^{-1}, indicating the significant variation in the radiative decay rates of the excited states. Strong transitions, such as those corresponding to the 22–0 and 26–0 transitions, show relatively large transition probabilities and oscillator strengths, signifying the presence of strong electric-dipole decay channels to the ground state. However, some transitions, for example, 48–0, show smaller transition probabilities and oscillator strengths, pointing to relatively weaker radiative decay pathways.

The oscillator strength f_{ji} for a transition is related to the radiative transition probability through a standard atomic-structure relation that involves the electron mass, charge, speed of light, statistical weights of the levels, and the transition wavelength. These parameters provide a quantitative description of the radiative characteristics of the atomic transitions and are broadly used in spectroscopic and plasma-diagnostic studies.

The oscillator strengths reported in Table 2 closely follow trends consistent with the calculated transition probabilities and line strengths. Transitions with the larger oscillator strengths correspond to the stronger radiative coupling between the upper and lower levels and therefore exhibit larger emission probabilities. Likewise, the line strengths offer an additional measure of the transition intensity and follow trends consistent with the corresponding oscillator strengths and transition probabilities.

Overall, the radiative parameters reported in Table 2 provide a reliable description of the electric-dipole transitions connecting the excited levels to the ground state of neon-like Se. These data play an important role in interpreting spectroscopic observations of highly charged ions and are also valuable for plasma diagnostics and modeling applications involving high-temperature laboratory or astrophysical plasmas.

Comparison with available reference data [15] confirms the reliability of the calculated wavelengths and radiative rates presented in Tables 3 and 4.

Table 3. Comparison of calculated wavelengths (in Å) for selected transitions in Ne-like Se with previously reported theoretical results [15].

I	J	λ (Å)	Ref [15]
2	0	8.632	8.623
4	0	8.391	8.383
16	0	7.979	7.975

Table 3. *Cont.*

I	J	λ (Å)	Ref [15]
22	0	7.881	7.877
26	0	7.693	7.690
30	0	7.284	7.287
32	0	7.234	7.237
38	0	6.380	6.377
46	0	6.245	6.242
48	0	6.232	6.229

Table 4. Comparison of calculated transition probabilities (A-values, s^{-1}) for selected transitions in Ne-like Se with previously reported theoretical results [15].

I	J	A_{IJ} (s^{-1})	Ref [15]
2	0	4.08×10^{12}	4.06×10^{12}
4	0	2.77×10^{12}	2.79×10^{12}
16	0	2.64×10^{11}	2.74×10^{11}
22	0	4.88×10^{13}	4.92×10^{13}
26	0	7.64×10^{13}	7.55×10^{13}
30	0	3.49×10^{12}	3.44×10^{12}
32	0	1.32×10^{13}	1.31×10^{13}
38	0	1.48×10^{12}	
46	0	1.69×10^{12}	
48	0	6.55×10^{10}	

3.4. Einstein Coefficients and Transition Characteristics

In addition to standard radiative parameters, we also evaluated Einstein coefficients for spontaneous and stimulated emission for the electric dipole transitions [16]. Table 5 lists the additional radiative parameters associated with electric-dipole transitions to the ground state of neon-like Se, which include the stimulated emission coefficient B_{ij}, ratio B_{ij}/A_{ij}, and transition dipole moment μ. These quantities provide deeper insight into the radiative coupling strength between the upper and lower levels.

Table 5. Einstein Coefficients for Spontaneous emission A_{IJ} (s^{-1}), Stimulated emission B_{IJ} ($m^3J^{-1}s^{-2}$), Transition dipole moment μ (Cm), for spectral lines of E1 transitions to ground state and corresponding emission and oscillator strengths for Ne-like Se.

S. No	J	I	Wavelength (m)	A_{IJ} (s^{-1})	Stimulated Emission Coefficient B ($m^3J^{-1}s^{-2}$)	B_{IJ}/A_{IJ} ($m^3J^{-1}s^{-1}$)	Transition Dipole Moment μ (Cm)	Emission Oscillator Strength F_{IJ}	Absorption Oscillator Strength (GRASP) F_{JI}
1	0	2	8.63×10^{-10}	4.08×10^{12}	1.58×10^{17}	3.88×10^{4}	3.04×10^{-31}	-4.61×10^{-2}	1.37×10^{-1}
2	0	4	8.39×10^{-10}	2.77×10^{12}	9.88×10^{16}	3.56×10^{4}	2.40×10^{-31}	-2.96×10^{-2}	8.78×10^{-2}
3	0	16	7.98×10^{-10}	2.64×10^{11}	8.10×10^{15}	3.06×10^{4}	6.89×10^{-32}	-2.55×10^{-3}	7.57×10^{-3}
4	0	22	7.88×10^{-10}	4.88×10^{13}	1.44×10^{18}	2.95×10^{4}	9.18×10^{-31}	-4.59×10^{-1}	1.36×10^{0}
5	0	26	7.69×10^{-10}	7.64×10^{13}	2.10×10^{18}	2.75×10^{4}	1.11×10^{-30}	-6.85×10^{-1}	2.03×10^{0}
6	0	30	7.28×10^{-10}	3.49×10^{12}	8.14×10^{16}	2.33×10^{4}	2.18×10^{-31}	-2.81×10^{-2}	8.33×10^{-2}
7	0	32	7.23×10^{-10}	1.32×10^{13}	3.02×10^{17}	2.28×10^{4}	4.20×10^{-31}	-1.05×10^{-1}	3.11×10^{-1}
8	0	38	6.38×10^{-10}	1.48×10^{12}	2.32×10^{16}	1.57×10^{4}	1.17×10^{-31}	-9.14×10^{-3}	2.71×10^{-2}
9	0	46	6.25×10^{-10}	1.69×10^{12}	2.49×10^{16}	1.47×10^{4}	1.21×10^{-31}	-1.00×10^{-2}	2.97×10^{-2}
10	0	48	6.23×10^{-10}	6.55×10^{10}	9.56×10^{14}	1.46×10^{4}	2.37×10^{-32}	-3.85×10^{-4}	1.14×10^{-3}

The calculated stimulated emission coefficients span several orders of magnitude, indicating the varying strengths of the corresponding electric-dipole transitions. Strong transi-

tions typically exhibit larger B_{ji} values and larger transition dipole moments. As an example, 0–26 and 0–22 transitions show the largest dipole moments, indicating strong electric-dipole coupling between the involved states. In contrast, transitions such as 0–48 show significantly smaller dipole moments, which correspond to weaker radiative coupling.

The ratio B_{ij}/A_{ij} lies within the expected range governed by the transition wavelength. The transition dipole moment additionally characterizes the strength of the interaction between the radiation field and the atomic system. Transitions with larger dipole moments exhibit stronger radiative coupling and thus contribute more prominently to the emission spectrum of the ion.

Overall, the additional parameters reported in Table 5 support the radiative transition probabilities and oscillator strengths. They provide a detailed description of the radiative properties of electric-dipole transitions in Neon-like Se.

4. Conclusions

We calculated transition wavelengths, transition probabilities, oscillator strengths, and line strengths for the lowest 50 fine-structure levels of highly charged neon-like selenium (Se XXV). We evaluated radiative transition rates for electric dipole, electric quadrupole, magnetic dipole, and magnetic quadrupole transitions among these levels.

The calculated excitation energies, wavelengths, oscillator strengths, and line strengths agree with values available in the NIST Atomic Spectra Database [14] and other published theoretical results [9,15]. This agreement supports the reliability of the relativistic treatment and the configuration interaction expansions used in the calculations.

For electric dipole transitions, we determined Einstein coefficients for spontaneous and stimulated emission, transition dipole moments, and both emission and absorption oscillator strengths. These parameters describe the radiative behavior of Ne-like Se XXV and support spectral modeling.

Our newly presented work is the determination of Einstein coefficients for spontaneous emission (A_{ij}, s^{-1}) and stimulated emission (B_{ij}, $m^3\ J^{-1}\ s^{-2}$), together with the corresponding transition dipole moments (μ, C·m). These quantities provide a complete and physically consistent description of radiative processes, since the transition dipole moment constitutes the fundamental quantity governing light–matter interaction and directly determines the magnitude of the Einstein coefficients and oscillator strengths.

The inclusion of both A_{ij} and B_{ij} allows us to describe not only spontaneous radiative decay but also induced emission processes that arise in the presence of external radiation fields. This distinction is essential in plasma environments where radiation fields are significant, such as in high-temperature laboratory plasmas, laser-produced plasmas, and astrophysical sources. In such systems, the stimulated emission coefficient (B_{ij}) plays a critical role in determining radiative balance and population kinetics, as it contributes directly to the rate equations governing level populations and modifies the net emission and absorption processes.

The transition dipole moment (μ) provides deeper physical insight by quantifying the strength of coupling between atomic states and the electromagnetic field. It directly governs transition probabilities, absorption coefficients, and spectral line intensities, and therefore plays a central role in the interpretation of emission and absorption spectra. Accurate values of μ are essential for calculating opacity, radiative cross sections, and line strengths, which are fundamental inputs in radiative transfer models and spectroscopic diagnostics.

By providing A_{ij}, B_{ij}, and μ simultaneously for Ne-like Se, the present work extends the available atomic dataset beyond standard radiative parameters and enables a more complete description of radiative processes. We derived radiative lifetimes for the lower excited levels from the total transition probabilities. The calculated lifetimes are consistent

https://doi.org/10.3390/psf2026013006

with the dominant allowed transitions and reflect the influence of relativistic and correlation effects in this highly charged ion. These results are particularly important for plasma modeling, where they support accurate simulations of level population dynamics, radiation transport, and energy balance, as well as for spectroscopic applications involving the determination of plasma temperature, electron density, and ionization conditions in both laboratory and astrophysical environments.

Author Contributions: Data curation, M.S.; formal analysis, M.S.; investigation, M.S.; methodology, R.P.; software, M.S.; supervision, R.S.; validation, M.S., R.P. and R.S.; visualization, M.S.; writing—original draft, M.S.; writing—review & editing, R.S., R.P. and M.S. All authors have contributed equally in performing calculations. All authors have read and agreed to the published version of the manuscript.

Funding: This research received no external funding.

Institutional Review Board Statement: Not applicable.

Informed Consent Statement: Not applicable.

Data Availability Statement: Data will be made available upon reasonable request.

Acknowledgments: We gratefully acknowledge the academic support and research facilities provided by Delhi Technological University.

Conflicts of Interest: The authors declare no conflict of interest.

References

1. Apruzese, J.P.; Davis, J. Enhancement of X-ray gain in neon-like ions by direct collisional pumping with suprathermal electrons. *Phys. Rev. A* **1983**, *28*, 3686–3688. [CrossRef]
2. Gupta, G.; Deb, N.; Msezane, A. R-Matrix Calculation of Electron Impact Excitation of Fine-Structure Levels of Ne-like Iron. *At. Data Nucl. Data Tables* **2000**, *74*, 257–266. [CrossRef]
3. Sugar, J.; Rowan, W.L.; Kaufman, V. Spectra of Se xvi to Se xxiv observed in a tokamak plasma. *J. Opt. Soc. Am. B* **1988**, *5*, 236–242. [CrossRef]
4. Stratton, B.C.; Hodge, W.L.; Moos, H.W.; Schwob, J.L.; Suckewer, S.; Finkenthal, M.; Cohen, S. Spectra of germanium and selenium in the 50–350-Å region from the PLT tokamak plasma. *J. Opt. Soc. Am.* **1983**, *73*, 877–881. [CrossRef]
5. Daido, H. Review of soft X-ray laser researches and developments. *Rep. Prog. Phys.* **2002**, *65*, 1513–1576. [CrossRef]
6. Li, R.; Liu, Y.; Mostamand, M.; Lassen, J. Resonance laser ionization spectroscopy of selenium. *Spectrochim. Acta Part B At. Spectrosc.* **2021**, *175*, 106017. [CrossRef]
7. Koch, J.A.; MacGowan, B.J.; Da Silva, L.B.; Matthews, D.L.; Underwood, J.H.; Batson, P.J.; Lee, R.W.; London, R.A.; Mrowka, S. Experimental and theoretical investigation of neonlike selenium X-ray laser spectral linewidths and their variation with amplification. *Phys. Rev. A* **1994**, *50*, 1877–1898. [CrossRef] [PubMed]
8. Osterheld, A.; Walling, R.; Young, B.; Goldstein, W.; Shimkaveg, G.; MacGowan, B.; Da Silva, L.; London, R.; Matthews, D.; Stewart, R. Ionization balance and gain calculations for neon-like selenium X-ray laser plasmas. *J. Quant. Spectrosc. Radiat. Transf.* **1994**, *51*, 263–271. [CrossRef]
9. Gupta, G.P.; A Berrington, K.; E Kingston, A. Electron impact excitation of neon-like selenium. *J. Phys. B At. Mol. Phys.* **1987**, *20*, L637–L639. [CrossRef]
10. Summers, H.P.; Behringer, K.; Wood, L. Recombination of Neon-like and Adjacent Ions in Plasmas. *Phys. Scr.* **1987**, *35*, 303–308. [CrossRef]
11. Abdallah, J.J.; Clark, R.E.H.; Peek, J.M. Steady-state ionization-balance calculations for a selenium plasma. *Phys. Rev. A* **1992**, *45*, 3980–3986. [CrossRef] [PubMed]
12. Dyall, K.; Grant, I.; Johnson, C.; Parpia, F.; Plummer, E. GRASP: A general-purpose relativistic atomic structure program. *Comput. Phys. Commun.* **1989**, *55*, 425–456. [CrossRef]
13. Gu, M.F. The flexible atomic code. *Can. J. Phys.* **2008**, *86*, 675–689. [CrossRef]
14. NIST Atomic Spectra Database (ver. 5.11). National Institute of Standards and Technology. Available online: https://www.nist.gov/pml/atomic-spectra-database (accessed on 17 March 2026).

15. Wang, K.; Chen, C.; Huang, M.; Wang, Y.; Zou, Y. Radiative rates and electron impact excitation rate coefficients for Ne-like selenium, Se XXV. *At. Data Nucl. Data Tables* **2011**, *97*, 426–480. [CrossRef]
16. Renk, K.F. Basis of the Theory of the Laser: The Einstein Coefficients. In *Basics of Laser Physics*; Springer: Berlin/Heidelberg, Germany, 2012; pp. 83–93. [CrossRef]

Disclaimer/Publisher's Note: The statements, opinions and data contained in all publications are solely those of the individual author(s) and contributor(s) and not of MDPI and/or the editor(s). MDPI and/or the editor(s) disclaim responsibility for any injury to people or property resulting from any ideas, methods, instructions or products referred to in the content.